Bull. Mater. Sci., Vol. 36, No. 6, November 2013, pp. 1037–1042. © Indian Academy of Sciences.

Aluminum alloy nanosecond vs femtosecond laser marking

S RUSU*, A BUZAIANU†, D G GALUSCA, L IONEL†† and D URSESCU††
Faculty of Materials Science and Engineering, Technical University "Gheorghe Asachi" of Iasi, No. 61A Dimitrie Mangeron Blvd., Iasi, Romania
†S.C. METAV-CD S.A., No. 31 C.A. Rosetti Street, Sector 2, Bucharest, Romania
††The National Institute for Laser, Plasma and Radiation Physics, No. 409 Atomistilor Street, Magurele, Bucharest, Romania

MS received 23 April 2012

Abstract. **Based on the lack of consistent literature publications that analyse the effects of laser marking for traceability on various materials, the present paper proposes a study of the influence of such radiation processing on an aluminum alloy, a vastly used material base within several industry fields. For the novelty impact, femtolaser marking has been carried out, besides the standard commercial nanosecond engraving. All the marks have been analysed using profilometry, overhead and cross-section SEM microscopy, respectively and EDAX measurements.**

Keywords. **Laser; marking; aluminum; nanosecond; femtosecond.**

1. Introduction

The modern industry, in order to preserve, protect, promote and enhance the value of their activities, use various methods of obtaining traceability characteristics, for preventing and reducing the forgery attempts, but also for the improvement of quality and safety of their products. Direct nanosecond laser (Kannatey-Asibu 2009) marking is a widely used flexible and modern method for obtaining permanent marks containing traceability and identification information: alpha-numeric strings of characters, logos, barcodes and data matrix codes. Femtosecond laser marking may bring consistent improvement in the visual and processing quality of the writing (Reif 2010), allowing micromachining with a very high precision, in particular for metals (Valette *et al* 2006). Regardless of the high quality of machining, the precision can be reduced by thermal and mechanical effects, but according to Lee *et al* (2010), compared to nanosecond laser sources, femtolasers have a lower ablation threshold and can spatially focus much more energy into the targeted substrate. Hence, undesired thermal effects are diminished, in order to obtain better-shaped structures.

The present work targets to identify and discuss the microstructural and functional differences between surfaces on which the two types of marking have been experimentally conducted, regarding that the literature on the surface behaviour of Al alloys is scarce for femtosecond laser treatment (Diels and Rudolph 2006; Sonntag *et al* 2009), not to mention on constructing a comparative analysis of the two engraving methods.

2. Experimental

The aluminum alloy used was determined to be of the Turbomecanica AU4G type for the aeronautic industry, equivalently 2017, used for forging highly resistant parts. It is a highly ductile alloy, with application temperatures ranging up to 175 and 250 °C for short usage. We determined a hardness of 14·4 HRC (144 HB) by using a Wilson Wolpert hardness meter and a standard main composition of 2·08% Cu, 2·17% Mg and 0·89% Fe, by applying EDAX analysis.

Marking was carried out using a Nd:YAG nanolaser: Trumpf VectorMark TruMark Station 1000 with a Trumpf VMC 1 laser (laser pulse wavelength: 1064 nm; beam mean power: 5·5 W; laser pulse energy: ∼0·5 mJ; repetition frequency: 10 kHz; laser pulse duration: 13–18 ns), respectively, a femtosecond laser: Clark CPA-2101 (laser pulse wavelength: 775 nm; beam mean power: 1·3–1·5 W; laser pulse energy: >700 μJ; repetition frequency: 2 kHz and laser pulse duration: ∼200 fs).

We marked 1 cm lines, for each type of laser. Regarding the 'commercial' nanolaser marking equipment, which used the vector marking principle, we also conducted superimposed laser scans by overlapping two passes of the beam. The obtained marks were analysed using Taylor Hobson profilometer, Quanta Inspect F scanning electron microscope (SEM) equipped with 1·2 nm resolution field emission gun (FEG) and 130 eV MnK resolution X-ray energy dispersive spectrometer (EDAX).

*Author for correspondence (rusu.st@gmail.com)

3. Results and discussion

3.1 *Overhead and cross-section SEM analysis of nanolaser marking*

SEM imaging shows the laser-engraved 10 mm long lines. One can notice the general roughness of the Al blade surface, in comparison to the one afferent to the mark segment, which is significantly more pronounced. Furthermore, figure 1 shows discontinuous and pulsed character of the laser treated line, composed from small areas of molten material. One can identify local melting of circular shape, subsequently solidified with partial superimposing of molten alloy. The laser writing presents a good directionality and an acceptably precise tendency to follow the blade's surface.

Upon exposure to laser radiation, the parameter which can qualitatively differentiate the two surfaces, marked and unmarked, is the R_k roughness factor (the roughness for the central part of the profile), afferent to the corresponding Abbott–Firestone curve (Abbott and Firestone 1933), which is 3·8 μm for a general R_a (profile mean arithmetic deviation) value of 1·27 μm (figure 2) inclusion. The width of the engraved segment ranges between 85 and 90 μm (figure 2), while the R_k parameter can be approximated with 10 μm, a considerably higher value in comparison to the previously obtained profilogram, but acceptable due to the constructive limitations of the equipment.

Superimposing the laser marks has been obtained by a double laser beam scan for the same coordinates. The results shown in figure 3 present a strong degradation of the exposed area, with massive deposits on each side of the mark, determined as Al and Mg oxides by means of the conducted EDAX analysis. The quantitative geometrical properties and the overall qualitative aspects can be established by the subsequent SEM images. The width of the mark does not exceed 90 μm, while R_k is ~15 μm.

We have cut the turbine blade in order to obtain a cross-section of the mark, in which one could analyse the lower part of the laser trace and base of the melt. The first aspect is that there are no induced cracks on any of the mark's surfaces visible in the cross-section. Figure 4 shows the solidification formations due to the thermal gradients resulting from the laser impact upon the blade surface. There are no microcracks or other types of defects determined by the material solidification thermal strains.

3.2 *Overhead and cross-section SEM analysis of femtolaser marking*

Based on the idea of high precision rapid marking of Al turbine blades, we applied ultra-short pulse processing, by means of femtosecond laser irradiation. In such applications, it is considered that there is no heat exchange between the beam and the target material (Huettner 2009; Kelton and Greer 2010). The ultra-fast modifications of the solid material can lead to the disappearance of thermally induced strains and compositional degradation.

The purpose of femtosecond pulsed laser processing was to avoid the formation of micrometric droplets, determined by the thermal effects from within the marked material, as seen in nanolaser engraving. Regarding that, the pulses have been below the picosecond scale, there is melting but no heat transfer. We are looking for a different behaviour of the marked alloy, with minimal heat diffusion, for a laser intensity below the ablation threshold.

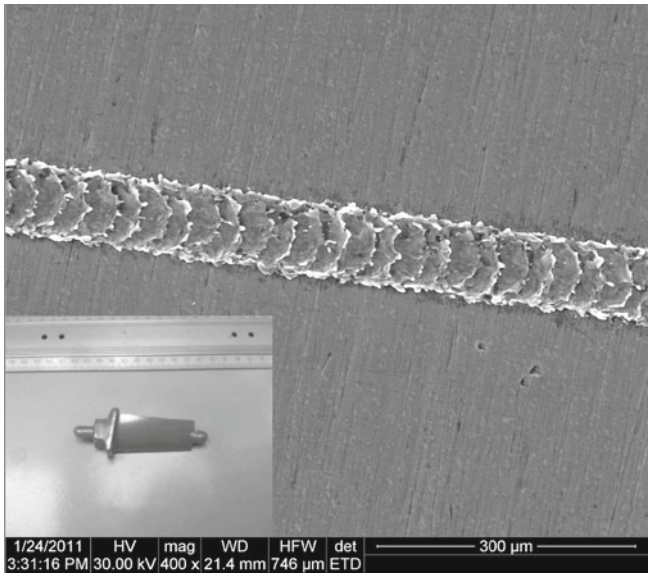

Figure 1. Mark's discontinuous and pulsed character, determined by formation of molten material areas (× 400). Figure includes an image of blade.

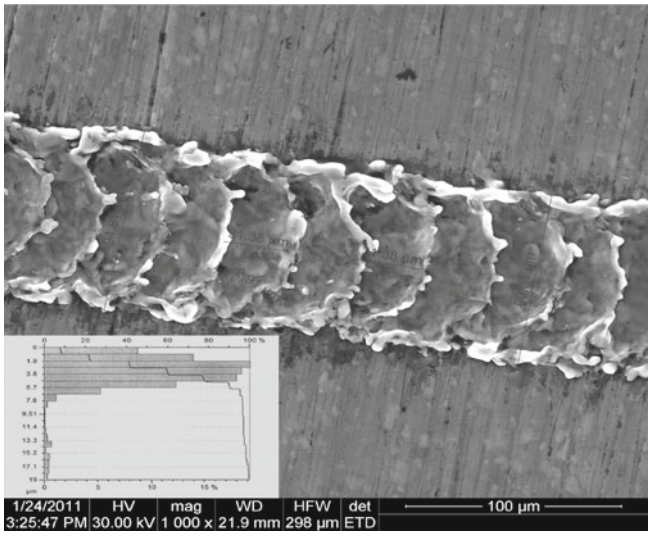

Figure 2. SEM image which shows a general view of nanolaser mark. Figure includes superimposing of Abbott–Firestone bearing area curve and surface roughness data.

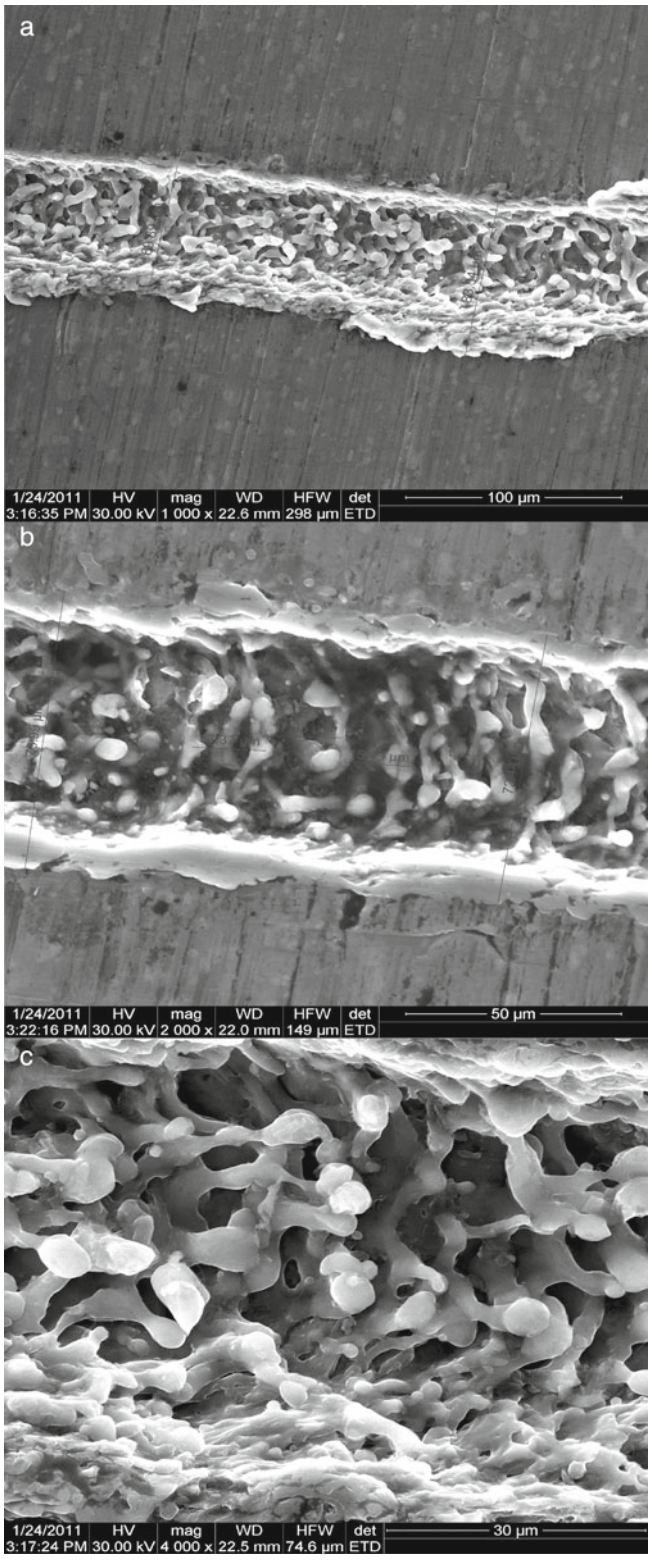

Figure 3. SEM micrographs of superimposed laser scans mark: (**a**) width of engraved segment and massive Al oxide deposits which follow scanning direction (× 1000); (**b**) molten material features and alloy dissipation within processed area, as droplets (× 2000) and (**c**) detail image showing ejected molten material from cavity and droplet form solidification of super-cooled Al alloy (× 4000).

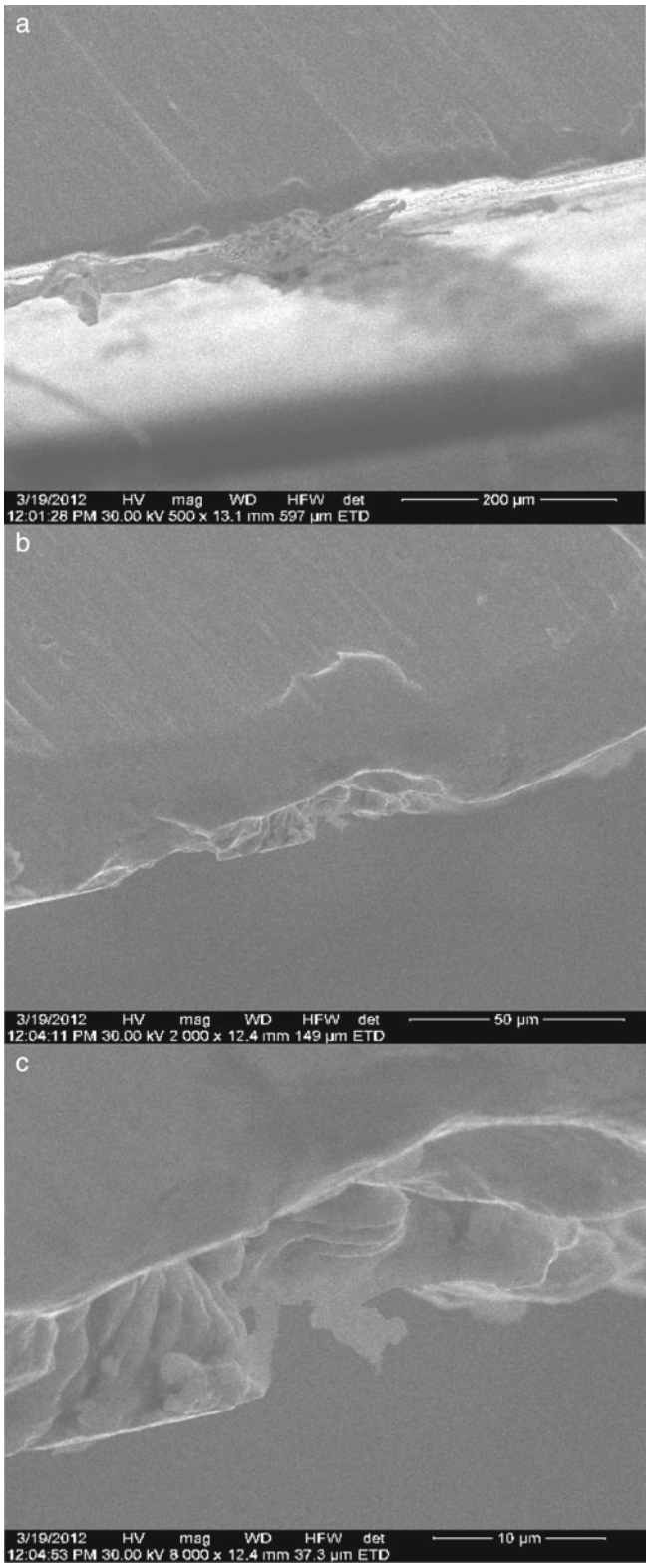

Figure 4. Mark cross-section SEM images: (**a**) general cross-section view of nanolaser mark (× 500); (**b**) profile of lower part of laser-created channel, which has a depth of ∼25 μm (× 2000) and (**c**) detail showing bottom profile and sidewalls of mark segment (× 8000).

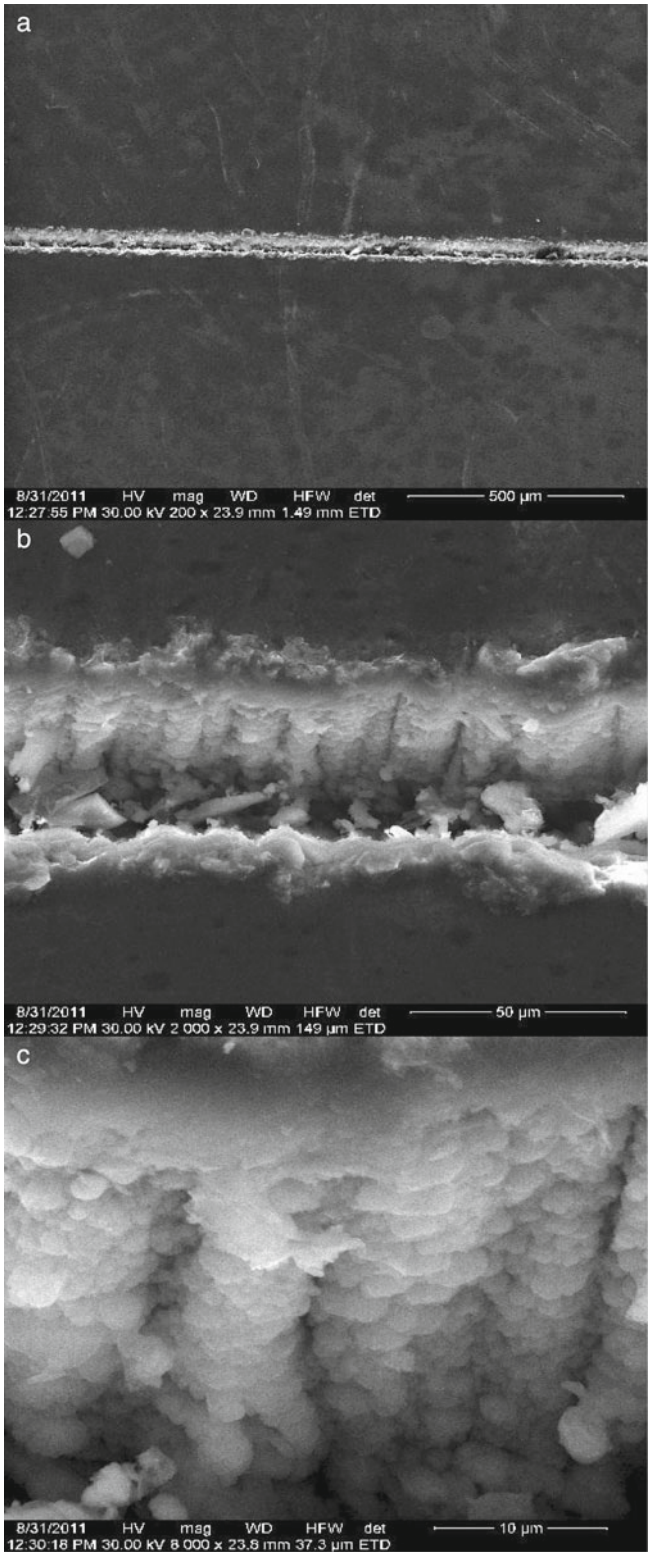

Figure 5. SEM micrographs of femtosecond laser mark: (**a**) general appearance of femtolaser mark, showing discontinuous and massive amorphous Al oxide deposits on each side of central molten area (× 200); (**b**) sidewalls of mark show a consistent depth of penetration (× 2000) and (**c**) details of solidification structure of sidewalls which bound channel (× 8000).

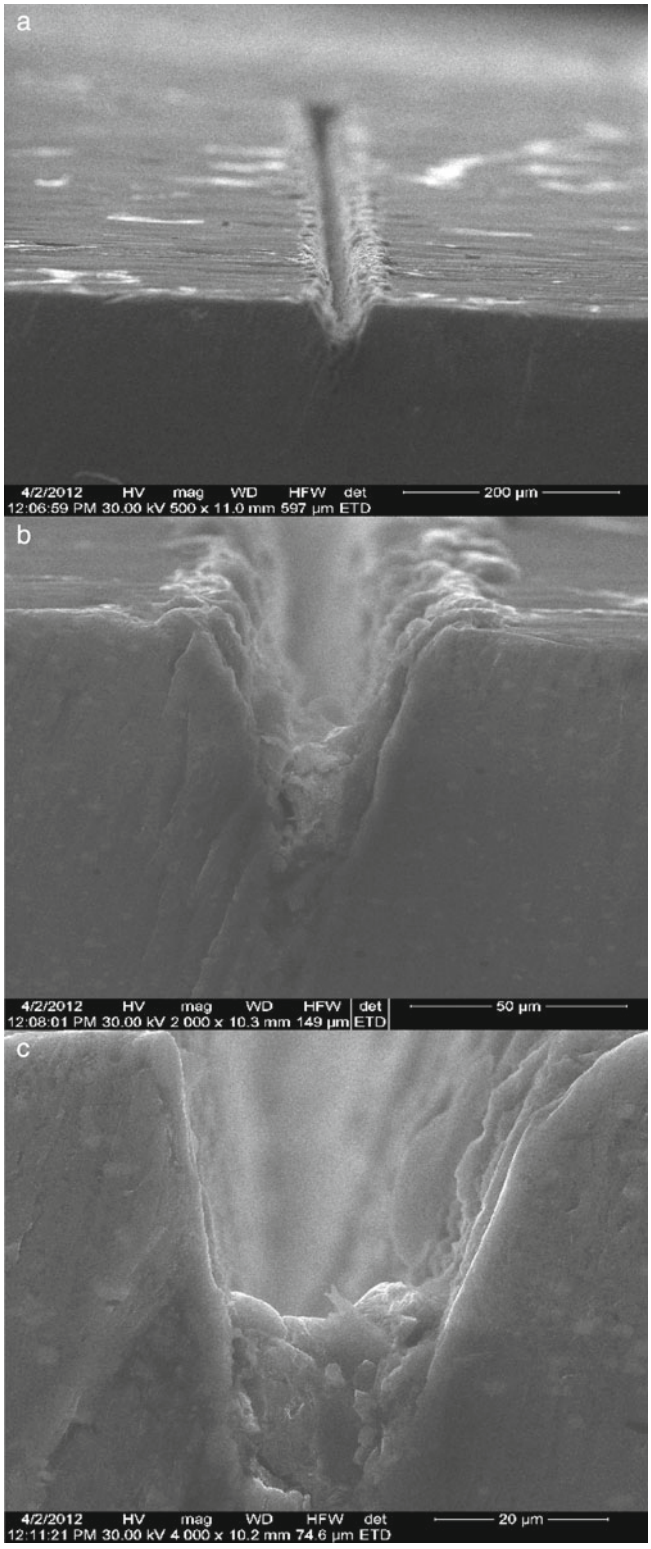

Figure 6. Cross-section SEM images of femtosecond laser mark: (**a**) general cross-section view of femtolaser mark (× 500); (**b**) sectioning profile and laser treatment resultant deposits (× 2000) and (**c**) detail showing bottom profile of mark segment. There are no cracks in analysed areas (× 4000).

One can notice that the obtained mark profile is continuous and of constant depth, with a completely different morphology than in the case of nano-second laser pulses. By means of SEM images presented in figure 5, the non-pulsed character of the engraved segment can be noticed, as well as the small adjacent amorphous structures of molten and ultra-rapidly solidified material. The melted channel is significantly narrower in comparison to its nanosecond version: 12–14 μm. A macroscopic view shows a total width of 70–75 μm, which also contains oxidized areas, composed of small local deposits of oxide particles, associated to the clearly limited thermally influenced areas.

A detailed analysis of the molten area indicates an in-depth penetration of the laser beam, which determined a distribution of the molten areas, followed by an ultra-fast solidification. The solidified areas are fragmented according to the scanning speed; this leads to the formation of rapid solidification structures, which present a vertical growth and are composed of conglomerates of spherical and amorphous particles, with a diameter of 0·5–2·5 μm.

These spherical formations, visible in figure 5(c), occur as a result of the molten micro-surface strong vibration within the laser beam; therefore, the freshly formed clusters of liquid alloy microspheres have the necessary thermodynamic conditions for an immediate ultrafast solidification, as this phenomenon takes place during just two consecutive laser pulses. They are determined to be compositionally homogeneous, by means of qualitative EDX imaging. The oxide layer makes the imagining different compared to the base materials and thus, these droplets appear "brighter".

As the femtolaser created channels are narrower and deeper than the ones corresponding to the nanolaser, the aforementioned profilometer limitations lead to the situation in which the measurement stylus cannot fit inside these marks. As we find ourselves in the innovating situation of conducting ultra-fast laser engraving, with high power equipment usually used for complex processing and melting, we have tried to find an optimal set up, in order to obtain the closest rate between the width and depth, in relation to the nanosecond laser marking.

To compensate for this situation, we have prepared cross-sections of the engraved segments for SEM analysis (figure 6).

The entire area from which the molten material has been eliminated is clearly visible in its depth; no important roughness modifications occur, except for a reduced area of deposits, of circa 5–8 μm, on each side of the marked groove. There is no cracking or any other type of induced defects.

4. Conclusions

In the case of nanosecond laser marks, due to the fact that the melting resulted from the laser beam scanning presents a very good stability and resistance to oxidation, high temperatures are reached only on the sample surface and for a depth which does not affect the functionality of the potential part (like a turbine blade, for instance). Mainly, the microstructure is not influenced, except for the superficial oxidation of certain elements.

The marking depth (respectively, the thickness of the alloy layer which presents structural modifications) obtained by employing laser treatment grows along with the laser beam power (for the same dimensions of the laser spot); the quality of the mark depends on the diameter of the laser spot, but also on the scanning speed. If the laser power exceeds 350 W, obvious irregularities occur. The conclusion regarding processing is that a mean scanning speed of 10 mm/s and 300–400 W laser beam can lead to a uniform mark, with a good texture and without massive oxide deposits.

We have shown that in the laser engraved areas, there is a slight oxidation of the exposed surface, while the texture is due to circular local melting, which has subsequently solidified, leading to partially super-imposed molten material areas.

When double-laser beam crosses have been conducted, with the same processing parameters as before, one can conclude upon the alteration of the quality characteristics of the mark. These quality variations are mainly due to micro-compositional and microstructural modifications within the laser re-melted areas. The induced structural defects are caused by the existence of an extremely high repetitive thermal gradient for the re-marked lines. By comparing the engraving characteristics, one can notice that the single-cross marks do not in any way affect the surface's quality and integrity.

Image analysis leads to the conclusion that the surfaces with the worst mark quality are the ones with double overlapping laser beam scanning. This can be explained by the fact that the mark formation time and the cumulated beam power are higher. At the same time, negative engraving effects occur, as the additional and repetitive temperature increasing in the marking area leads to more oxide deposits.

For femtosecond laser engraving, there is a completely different morphology, with a more continuous marking profile, of a more constant depth and with a well-defined outline. In the marked areas, re-crystallization areas are absent, except small amorphous oxide fragments. A detailed analysis of the molten area has indicated an in-depth penetration of the laser beam, with a clear separation into melting and ultra-fast solidification areas. The solidification zone is fragmented with regard to the beam surface scanning speed. The molten areas copy the geometry of the laser spot and maintain the sequential character and rapid solidification property of the beam scanning upon the alloy surface.

There is a far superior uniformity and continuity to the molten and then ultra-fast solidified alloy, especially on the walls of the mark; the "cut" obtained by melting is far more homogenous. Rapid solidification structures are formed with a vertical growth, composed of 'conglomerates' of spherical particles, with an amorphous structure. The laser beam creates a narrow marking area, which is delimitated on each side

of the melt by oxide deposits with fragmentary deposition and depositing.

From a quantitative point of view, all undertaken analyses show that no modifications have occurred. The difference stands in certain qualitative issues, which have been approached closely. In conclusion, despite the proven fact that femtosecond laser marking is superior from the qualitative point of view given by microscopic imaging, the proven benefits do not tip the scales in its favour, because of the technological costs and sheer applicable dimensions of the apparatus itself.

Acknowledgement

This paper was realized with the support of EURODOC "Doctoral Scholarships for research performance at European level" Project, financed by European Social Fund and Romanian Government.

References

Abbott E J and Firestone F A 1933 *Mech. Eng.* **55** 569

Diels C and Rudolph W 2006 *Ultrashort laser pulse phenomena—fundamentals, techniques and applications on a femtosecond time scale* (Elsevier) pp. 544–549

Huettner B 2009 *The theory of laser materials processing* (ed.) J Dowden (Springer) in *Femtosecond laser pulse interactions with metals*, p. 315

Kannatey-Asibu Jr E 2009 *Principles of laser materials processing* (New Jersey: John Wiley & Sons) pp. 409–427 and 568–594

Kelton K F and Greer A L 2010 *Pergamon Mater. Series* **15** 511

Lee C Y, Chang T C, Wang S C, Chien C W and Cheng C W 2010 *Biomicrofluidics* **4** 046502

Reif J 2010 *Laser-surface interactions for new materials production* in *Basic physics of femtosecond laser ablation* (eds) A Mitello and P M Ossi (Berlin Heidelberg: Springer-Verlag) pp 19–43

Sonntag S, Roth J, Gaehler F and Trebin H R 2009 *Appl. Surf. Sci.* **255** 9742

Valette S, Le Harzic R, Audouard E, Huot N, Fillit R and Fortunier R 2006 *Appl. Surf. Sci.* **252** 4691